Performances and Design Studies Status of the P4S-1 Thruster

H. Brito[&], S. Elaskar[+&], C. Brito[*] and R. Ballete[+]

[&]Instituto Universitario Aeronáutico,
Av. Fuerza Aérea Argentina, km 5.5, (5016) Córdoba, Argentina.

[+]Departamento de Aeronáutica, Universidad Nacional de Córdoba,
Av. Velez Sarfield 1600, (5000) Córdoba, Argentina.

*ENSAE, Toulouse, France

e-mail: hbrito@make.com
e-mail: selaskar@com.uncor.edu

IEPC-01-145

A new model to calculate the ablated mass and the impulse bit of ablative plasma pulsed thrusters (APPT) is presented throughout this paper. The model is based on the balance of energies involved in APPTs way of working. A new expression is obtained for the ablated Teflon mass as a function of the main electric and geometric parameters. The introduction of an ideal arc thickness allows to define a simplified model useful for the prediction of the performances and for preliminary design activities. The obtained theoretical results about the impulse bit show good agreement with those arising from experimental studies. A comparison is carried out on five APPTs; the relative error is approximately equal to 10%. Finally, this new model is used to evaluate the ablated mass of the P4S-1 thruster being currently under development in Argentina.

Introduction

The ablative plasma pulsed Teflon thrusters (APPT) are very convenient propulsion devices for applications to orbit maintenance, attitude control and in-flights formations, due to their ability to produce small impulse bits with high specific impulses [1]. The use of Teflon (as propellant) permits the additional benefit of safety and compact design [2].

The APPT show in Fig. 1 starts its operation cycle when the Processing Power Unit (PPU) takes power from the satellite bus and loads the capacitor bank at a voltage V_0. The Teflon bar is fed between a couple of electrodes that are connected to the capacitors. An ignition spark plug is fired producing enough electric conductivity inside the acceleration chamber as to allow the capacitors to liberate the accumulated energy thus leading to the Teflon ablation. The electric current flows from the capacitors through the acceleration electrodes and the arc, forming a current loop which induces a magnetic field. A few microscopic sheets of the Teflon surface are ionized and accelerated by the Lorenz forces due to the interaction between the arc and the induced magnetic field. An important fraction of the ablated mass is neutral being accelerated by gasdynamics effects. Therefore, the ablated mass is accelerated by a combination of gasdynamic and electromagnetic forces. Once the capacitor bank is discharged, the cycle resumes giving shape to the pulsed behavior.

The final design of an APPT device requires the use numerical simulation due to the complex interrelations between electric, geometric, gasdynamics, magnetogasdynamics phenomena and the non-steady mechanism of arc formation [3,4].

Some models of electric discharge are based on the solution of time dependent equation systems taking place when energy balance, thermal conductivity, Teflon ablation and mass conservation are considered. These models are complete enough to give a functional description of the APPT; unfortunately, they are usually based on a particular geometric configuration and the extension of their use to another geometry is not immediate. There are empirical models based on ablation functions for different geometric configurations. These models use the interpolation of experimental data and the accuracy of them is restricted to APPTs working in conditions similar to those of the experiments [5-8].

A new theoretical relationship linking the ablated mass with the main electric and geometric parameters is presented in this paper. To obtain the main equation the energy balance involved in generation and transport of the current pulse, in arc generation, in heat dissipation and in plasma acceleration is considered. The introduction of an ideal arc thickness in the descriptive equations allows to build up a simplified model useful for the preliminary design of an APPT.

Finally the found analytical relationship is applied for the preliminary evaluation of the P4S-1 thruster ablated mass. P4S-1 is an APPT being currently under development in Córdoba, Argentina.

Analytical model for the prediction of the ablated mass

In this section the new theoretical model is displayed and applied for the calculation of the ablated mass and the impulse bit. With the aim of building a simple analytical model the following assumptions are introduced:

Assumption 1: The new model is based on a zero-dimensional analysis (global quantities).

Assumption 2: The energy balance starts at the capacitor bank, because this device governs the discharge time. Another aspect to be considered is that the capacitors bank is the first place in which energy losses are important [9].

Assumption 3: From an electric circuit point of view the acceleration chamber, the electrodes and the plasma are active components of a RLC circuit with constant parameters. This idealization allows to consider the plasma as a conductor with resistance and inductance [10], and to define the electromagnetic impulse associated to ion acceleration [11].

Assumption 4: The heat losses during the ablation process are calculated considering heat transfer by black body radiation only. It is important to notice that the energy distribution in the plasma is due to combined radiation and convection effects [5], however convection can be neglected when the pressure in the APPT is higher than 1 hbar [11,12].

Assumption 5: It is accepted, according to Ref. [11] that the necessary specific energy for Teflon ablation is 1.5×10^6 J/kg. This value includes the specific energy for the breakdown of Teflon polymer chains. On the other hand, the ionic and neutral mass are supposed respectively equal to $m_i = (0.1 \pm 0.05)m$ and $m_n = (0.9 \quad 0.05)m$. However, Spanjers *et al*. [13] found m_i/m values up to 0.25.

Assumption 6: The plasma is confined within a volume at homogeneous temperature and the interactions among the particles lead to thermodynamic equilibrium [5].

Assumption 7: The neutral mass expands as a perfect gas in a subsonic cavity. The volume of this

cavity is that of the acceleration chamber. The highest gas velocity will be the sonic velocity.

Energy Balance Inside of an APPT

The energies involved in an APPT are shown in Fig. 2. The energy balance can be expressed as:

$$E_o = E_{joule} + E_{sh} + E_{heat} + E_{gas} + E_{em} + E_{et} \tag{1}$$

E_0 is the energy stored in the capacitors, E_{joule} represents the energy losses by Joule effect, E_{sh} is the energy at the potential sheaths, E_{heat} represents the energy loss by heat dissipation, E_{gas} is the energy needed to ablated the Teflon, E_{em} is the electromagnetic energy and E_{et} is the energy associated to gasdynamics effects. The three RHS first terms are energy losses, and they do not contribute to the impulse. However, the last three RHS terms are ablated mass dependent. Therefore, the energies involved in the right side of Eq. (1) can be written in terms of the efficiencies and/or ablated mass. The objective is to obtain an equation that links the ablated mass, the efficiencies associated to the energy accumulated in the capacitors, the ohmic losses due to imperfect conductors, the voltage losses in the potential sheaths, the heat dissipation in the arc and the velocity losses in the plasma due collisions between particles. Eq. (1) can be written as a function of the ablated mass in the following form:

$$E_o = (1-\eta_{trans})E_o + (1-\eta_{sh})\eta_{trans}E_o + (1-\alpha_A)(\eta_{trans}\eta_{sh}E_o - E_{em}) + me_{gas} + C_{em}\frac{E_o^2}{m} + \frac{m}{C_{et}} \tag{2}$$

where

$$\eta_{trans} = \frac{R_{PPT}}{R_{tot}}, \qquad \eta_{sh} = \left(1 + \frac{(V_{sh})_{max}}{I_{max}R_{PPT}}\right)^{-1},$$

$$C_{em} = \frac{1}{8\alpha_i\eta_{fi}}\left(\frac{L'_{PPT}}{R_{tot}}\right)^2, \qquad C_{et} = \frac{(1-\eta_{fn})^2(\gamma-1)^2}{2\alpha_n\eta_{fn}a^2}$$

and α_i, α_n are the ratios between ionized mass and neutral mass and the total ablated mass respectively.

Following some algebra manipulation Eq. (2) can be rewritten as:

$$\left(e_{gas} + C_{et}^{-1}\right)m^2 - \alpha_A\eta_{trans}\eta_{sh}E_o m + \alpha_A C_{em}E_o^2 = 0 \tag{3}$$

By solving the last expression for the ablated mass one can obtain

$$m = \frac{\alpha_A \eta_{trans} \eta_{sh} E_o \pm \sqrt{(\alpha_A \eta_{trans} \eta_{sh} E_o)^2 - 4\alpha_A C_{em} E_o^2 (e_{gas} + C_{et}^{-1})}}{2(e_{gas} + C_{et}^{-1})} \quad (4)$$

Eq. (4) should have an unique solution on physical grounds. The ablated mass can then be expressed as:

$$m = \frac{\alpha_A \eta_{trans} \eta_{sh} E_o}{2(e_{gas} + C_{et}^{-1})} \quad (5)$$

Introduction of the ideal arc thickness

The following assumption completes the group listed at the beginning of this paper; it allows to estimate some necessary electric and geometric parameters.

Assumption 8: The geometry of the arc is supposed simple and confined within the acceleration chamber. The use of this last assumption allows to estimate the plasma resistance R_{PPT}. This resistance will depend on the acceleration chamber and electrodes geometries. For example, for the APPT show in Fig. 1 one has

$$R_{PPT} \cong R_{plasma} = \eta h / w\delta$$

where δ is the arc ideal thickness and η is the plasma resistivity. The total resistance of the circuit shown in Fig. 3 is expressed as a function of the arc ideal thickness. Consequently, the arc temperature, the frozen flow efficiencies and the sound velocity are also dependent of the parameter δ.

It is important to notice that, without regard to the type of the Teflon bar feeding and the electrodes geometry, is in general possible to express the radiation area as a function of the Teflon exposed area, the dimensions of the acceleration chamber and the arc thickness. For example, for the APPT shown in Fig. 1 is

$$A_{rad} = 2A_p + 2\delta(w+h)$$

Thus, it is possible to calculate α_A. To determine the ablated mass, the only parameters independent of the arc thickness are the inductance gradient L'_{PPT}, the energy of the capacitor bank E_o and the constants η, γ, α_i and e_{gas}. The process of evaluation of the ablated mass is shown in Fig. 4. However, for each APPT the evaluation of A_p, A_{rad}, R_{plasma} and L'_{PPT} .will be needed.

Comparison with experimental results

In order to verify the ability of this new model for the prediction of preliminary performances, it is applied to five APPTs: the OSU/LeRC Benchmark PPT [18], the Les-6 [3, 4], the XPPT-1 [13], the APPT given in Ref. [19] and the PPT-4 [14].

Table 1 shows the electric and geometric parameters for this five APPTs. The three first APPTs have a two-dimensions configuration with parallel electrodes. The APPT described in Ref. [19] has a two-dimension geometry but with two lateral Teflon bars as feeding system, and the electrodes have a 20 degrees divergence angle. The PPT-4 configuration is a coaxial one as shown in Fig. 5, where two springs feed laterally two Teflon bars among insulators of boron. Assuming that the plasma develops geometrically according to that indicated in Fig. 5; the plasma resistance can be estimated as

$$R_{plas} = \eta l_i / \pi d_m \delta$$

where l_i is the arc length and d_m is the average diameter between d_{Teflon} and d_{an}. Approximately

30% of the inner cavity area corresponds to insulators, so the exposed Teflon area is

$$A_p = 0.70\,\pi\, d_{cav}\, l\,.$$

For the first three APPTs with two-dimension geometry, the Teflon feeding is done from behind and the inductance of the system (electrodes + potential sheaths + plasma) writes [20]

$$(L_{PPT})_{rect} = 0.4\, l\left(\ln\left[h/(e+w)\right] + 0.22(e+w)/l - h/l + 1.5\right)$$

For the APPT of Ref. [19] with lateral feeding, the inductance is

$$(L_{PPT})_{rect} = \mu_o h l / w$$

According to Refs. [3, 11, 14], the inductance of APPTs with coaxial geometry is expressed as

$$(L_{PPT})_{coax} = (\mu_o l / 2\pi)\left[0.25 + \ln(r_a / r_c)\right]$$

The plasma resistivity can be considered that of a Lorenz gas using the factor γ_E which takes into account the electron-electron collisions in a partially ionized gas; for Z = 2, γ_E = 0.683 [22]. For plasma temperatures of approximately 2 eV and densities between 10^{21} m^{-3} and 10^{24} m^{-3}, the averaged resistivity of a doubly ionized plasma can be taken as 2×10^{-4} Ωm, coincidentally with the calculations carried out on the APPT from Refs. [5] and [23]. Refs. [11, 14 and 24] use for the specific heat ratio a value between 1.3 and 1.4. However, if the temperature is in the range 1 to 2 eV and density from 10^{21} m^{-3} to 10^{24} m^{-3}, it is possible to assume that the molecules of C_2F_4 have been completely dissociated [25]. The neutral particles will then only have three degrees of freedom, which implies γ = 1.67.

The values of ablated mass and impulse bit obtained with the new model are compared in Table 2 with those published in the aforementioned references. In all calculations a specific heat ratio equal to 1.67 has been used, and the assumption was made that the ionic mass amounts to 10% of the total ablated mass. However, it can be observed that adopting α_i=0.25 for the XPPT-1, according to measures carried out by Spanjers *et al*. [13], the prediction of the ablated mass improves remarkably, the obtained value being 26.8 μg (e_m = -6%). Likewise if for the PPT-4 one takes γ = 1.3, as indicated in Ref. [11], the ablated mass and the impulse bit become 43.9 μg and 301 μNs with the following error figures, respectively: e_m = -2.5% and e_I = 19.5%.

Application to the P4S-1 thruster

The preliminary performances evaluation of P4S-1 is presented in this section.

The P4S-1 is an APPT thruster that is being developed in Argentina. Presently, the geometry of this thruster is cylindrical with coaxial electrodes. The feeding device consists of a spring that push the Teflon bar between the electrodes. The electrodes length is 30mm.

Operational requirements of the thruster are:

- Total impulse: 10,000 Ns.
- Average Thrust: 0.5 mN
- Number of cycles: less than 30,000,000.
- Bus Power: less than 50 watts.

The results furnished by the analytical model are displayed in two dimensional pictures. These pictures have in the horizontal axis the operational voltage and in the vertical axis the capacity of the capacitor bank. For example, Fig. 6 shows a typical picture used to study the performances of P4S-1. In this figure the mass, the bus power and the number of pulses as functions of the voltage and the capacity, are shown. One can observe that the conditions imposed by the number of pulses and the

bus power are satisfied within a certain region of the graph.

Since the ratio between ionic mass with ablated mass (α_i) and the specific heat ratio (γ) are not exactly known, the thruster behavior is analyzed for the ranges:

$$0.1 \le \alpha_i \le 0.2$$

$$1.28 \le \gamma \le 1.67$$

Each pair α_i-γ defines a picture similar to Fig. 6. The next step is to find the intersection region satisfying both the number of pulses and the bus power constraints, in the voltage-capacity figure and considering all studied cases. This region is the more conservative situation as far as the evaluation of the total mass of the thruster is concerned. This intersection region is shown in Fig. 7. Finally, the minimum P4S-1 total mass is found to be 7.45 kg.

Conclusions

The model presented in this paper permits to evaluate the main performances of an APPT (specific impulse, propulsive efficiency and ablated mass per pulse). The model has been found to be an useful tool for the preliminary design of APPTs. The wide spectrum of variables considered by the model allows to approach in a quite complete way this kind of design activity. For instance, the model is able to estimate energy losses due to heat dissipation, the average value of the temperature developed in the plasma and the maximum currents developed during the discharge. The comparison of the values calculated by using the model with experimental data corresponding to five APPTs gives the following average values of the relative error: -40% for the ablated mass and 10% for the impulse bit. In spite of the order of magnitude of the existent differences between the calculated values and the experimental ones, the application of the model can be advantageous, keeping in mind that by using empiric ablation functions higher relative errors are obtained. The model possesses the following additional advantages: to allow a sensitivity study of performances; to permit the incorporation of more developed sub-models like the theoretical simulation of different combinations of electric-geometric parameters.

Finally, the new model was used to calculate the ablated mass and the total mass for the P4S-1 thruster. This is a preliminary evaluation, however it is important for assessing the influence of different parameters, being a first step before considering more sophisticated simulations.

Acknowledgements

This work has been supported by means of grants PICT-99-10-07107 of Argentina's National Agency for the Support of Science and Technology and 05-M026 of National University of Cordoba. Support provided by a grant from Cordoba Science Agency is also acknowledged.

References

1) Myers, R. M., Cassady, R. J., "Overview of Major U.S. Industrial Programs in Electric Propulsion," AIAA Paper 98-3179, 1998.

2) Rayburn, C., Campbell, M., Hoskins, W., Cassady, R., "Development of a Micro Pulsed Plasma Thruster for the Dawgstar Nanosatellite," AIAA Paper 2000-3256, 2000.

3) Turchi, P. J., Mikellides, I. G., Mikellides, P. G., Schmahl, C. S., "Theoretical Investigation of Pulsed Plasma Thrusters," AIAA Paper 98-3807, 1998.

4) Mikellides, P. G., Turchi, P. J., "Modeling of Late-Time Abaltion in Pulsed Plasma Thrusters," AIAA Paper 96-2733, 1996.

5) Keidar, M., Boyd, I. D., Beilis, I. I., "A Model of an Electrical Discharge in a Coaxial Pulsed Plasma Thruster," IEPC Paper 99-214, 26th International Electric Propulsion Conference, Kitakyushu, 1999.

6) Guman, W. J., "Designing Solid Propellant Pulsed Plasma Thrusters," AIAA Paper 75-410, 1975.

7) Rudikov, A. I., Antropov, N. N., Popov, G. A., "Pulsed Plasma Thruster of Erosion Type for a Geostationary Artificial Earth Satellite," IAF Paper 93-S.5.487, 44th Congress of the International Astronautical Federation, Graz, 1993.

8) Ziemer, J. K., Choueiri, E. Y., Jahn, R. G., "Scaling Laws for Pulsed Electric Propulsion with Application to the Pluto Express Mission," Electric Propulsion and Plasma Dynamics Laboratory, Princenton University.

9) Chen, Z., Brandhorst, H., "Performance of High Power Capacitors for Pulsed Plasma Thruster Applications," IEPC Paper 99-060, 26th International Electric Propulsion Conference, Kitakyushu, 1999.

10) Vondra, R. J., Thomassen, K., "Flight Qualified Pulsed Electric Thruster for Satellite Control," *Journal of Spacecraft and Rockets*, Vol. 11, No. 9, 1974, pp. 613-617.

11) Burton, R. L., Wilson, M. J., Bushman, S. S., "Energy Balance and Efficiency of the Pulsed Plasma Thruster," AIAA Paper 98-3808, 1998.

12) Church, C. H., Schlecht, R. G., Liberman, I., Swanson, B. W., "Studies of Highly Radiative Plasma Using the Wall-Stabilized Pulsed Arc Discharge," AIAA Journal, Vol. 4, No. 11, 1966, pp. 1947-1953.

13) Spanjers, G. G., McFall, K. A., Gulczinski, F. S., Spores, R. A., "Investigation of Propellant Inefficiencies in a Pulsed Plasma Thruster," AIAA Paper 96-2723, 1996.

14) Bushman, S. S., Burton, R. L., Antonsen, E. L., "Arc Measurements and Performances Characteristics of a Coaxial Pulsed Plasma Thruster," AIAA Paper 98-3660, 1998.

16) Delcroix, J. L., "Introduction a la théorie des gaz ionisés," Monographies Dunod, Dunod, Paris, 1959.

17) Sutton, G., Sherman, A., "Engineering Magnetohydrodynamics," 1st ed., McGraw-Hill, New York, 1965.

18) Kamhawi, H., Turchi, P. J., Leiweke, R. J., Myers, R. M., "Design and Operation of a Laboratory Benchmark PPT," AIAA Paper 96-2732, 1996.

19) Palumbo, D. J., Guman, W. J., "Effects of Propellant and Electrode Geometry on Pulsed Ablative Plasma Thruster Performance," AIAA Paper 75-409, 1975.

20) Anderson, H. L., (ed.), "Physics Vade Mecum," American Institute of Physics, New York, 1981.

21) Jahn, R. G., "Physics of Electric Propulsion," Mc Graw-Hill Book Co., New York, 1968.

22) Spitzer, L., Jr., "Physique des gaz completement ionisés," Monographies Dunod, Dunod, Paris, 1959.

23) Eckman, R., Byrne, L., Cameron, E., Gatsonis, N. A., Pencil, E., "Triple Langmuir Probe Measurements in the Plume of a Pulsed Plasma Thruster," AIAA Paper 98-3806, 1998.

24) Turchi, P. J., Leiweke, R. J., Kamhawi, H., "Design of an Inductively-Driven Pulsed Plasma Thruster," AIAA Paper 96-2731, 1971.

25) Curran, F. M., Myers, R. M., Rudolph, L. K., Wilbur, P. J., "Electric Propulsion for Space Systems," *An AIAA Professional Development Short Course*, Cleveland, Ohio, July 16-17, 1998.

26) Mikellides, I. G., Turchi, P. J., "Optimization of Pulsed Plasma Thrusters in Rectangular and Coaxial Geometries," IEPC Paper 99-211, 26th International Electric Propulsion Conference, Kitakyushu, 1999.

Table 1. Electric and geometric parameters of five APPTs

	OSU/LeRC	LES-6	XPPT-1	PPPA (Ref. 1)	PPT-4	
Geometry	*BF* (rect.)	*BF* (rect.)	*BF* (rect.)	*SF* (rect.)	*SF* (coaxial)	
C, μF	10	2	10	9	8	
V_o, kV	1.415	1.36	2.24	10	1.5	
R_{ext}, mΩ	16	30	50	10.1	8.5	
L_{ext}, nH	116	34	50	70	75	
l_{an}, mm	38.1	60	100	41	l, mm	25
l_{cat}, mm	44.5	60	100	41	d_{cav}, mm	6.4
e, mm	6.4	3	5	-	d_c, mm	4.8
h, mm	25.4	30	25	66	d_a, mm	43
w, mm	25.4	10	25	9.5[a]	$a_{exp.aisl}$	30%

[a]In this case w is the distance between the two Teflon bars. The Teflon is laterally fed. The width of electrodes is 38 mm.

Table 2. Main performances and relative error in the ablated mass and the impulse bit

	OSU/LeRC	LES-6	XPPT-1	PPPA	PPT-4
m, μg	11.6	10	28.5	1780	45
I, μNs	-	31.2	279.5	17000	252
m_{pred}, μg	32.9	4.3	38.3	2846	87.2
I_{pred}, μNs	149.1	22.4	178.3	16200	358.3
e_m, %	183.9	-56.4	34.4	59.9	93.8
e_I, %	-	-28.2	-36.2	-4.7	42.2

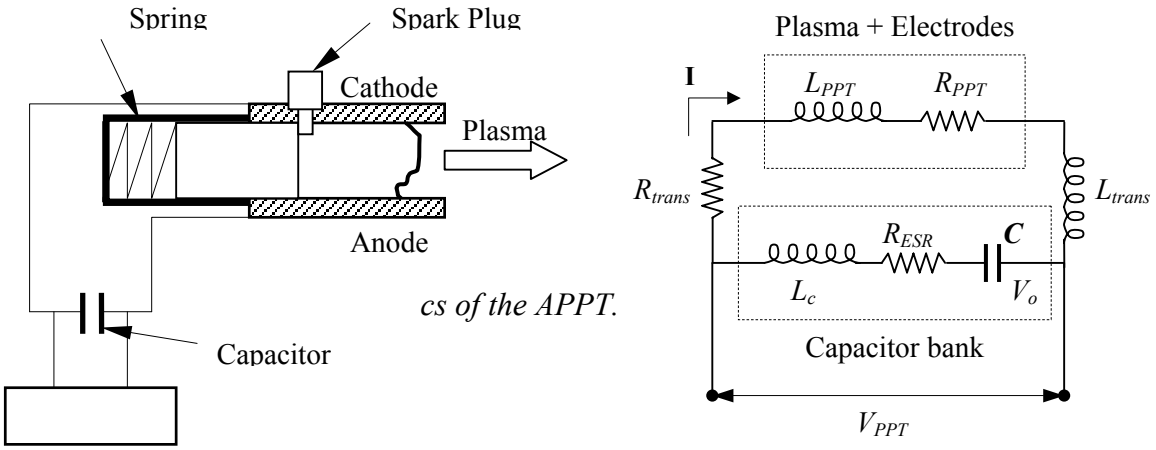

Figure 1. Outline and idealized electronic

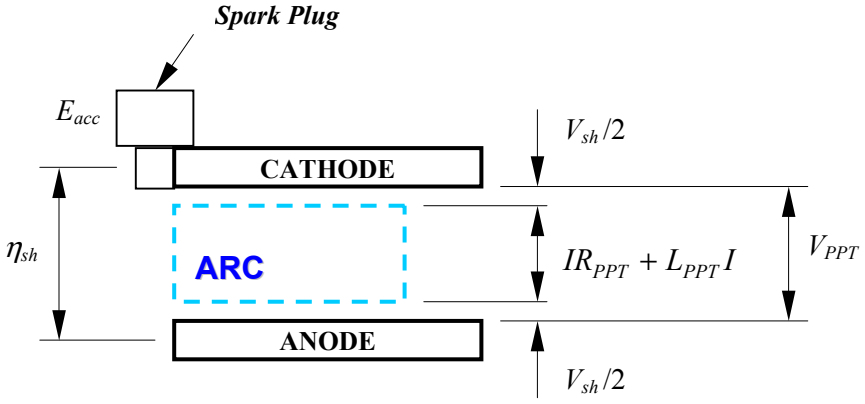

Figure 3. The η_{sh} determination as a function of voltage losses at the potential sheaths.

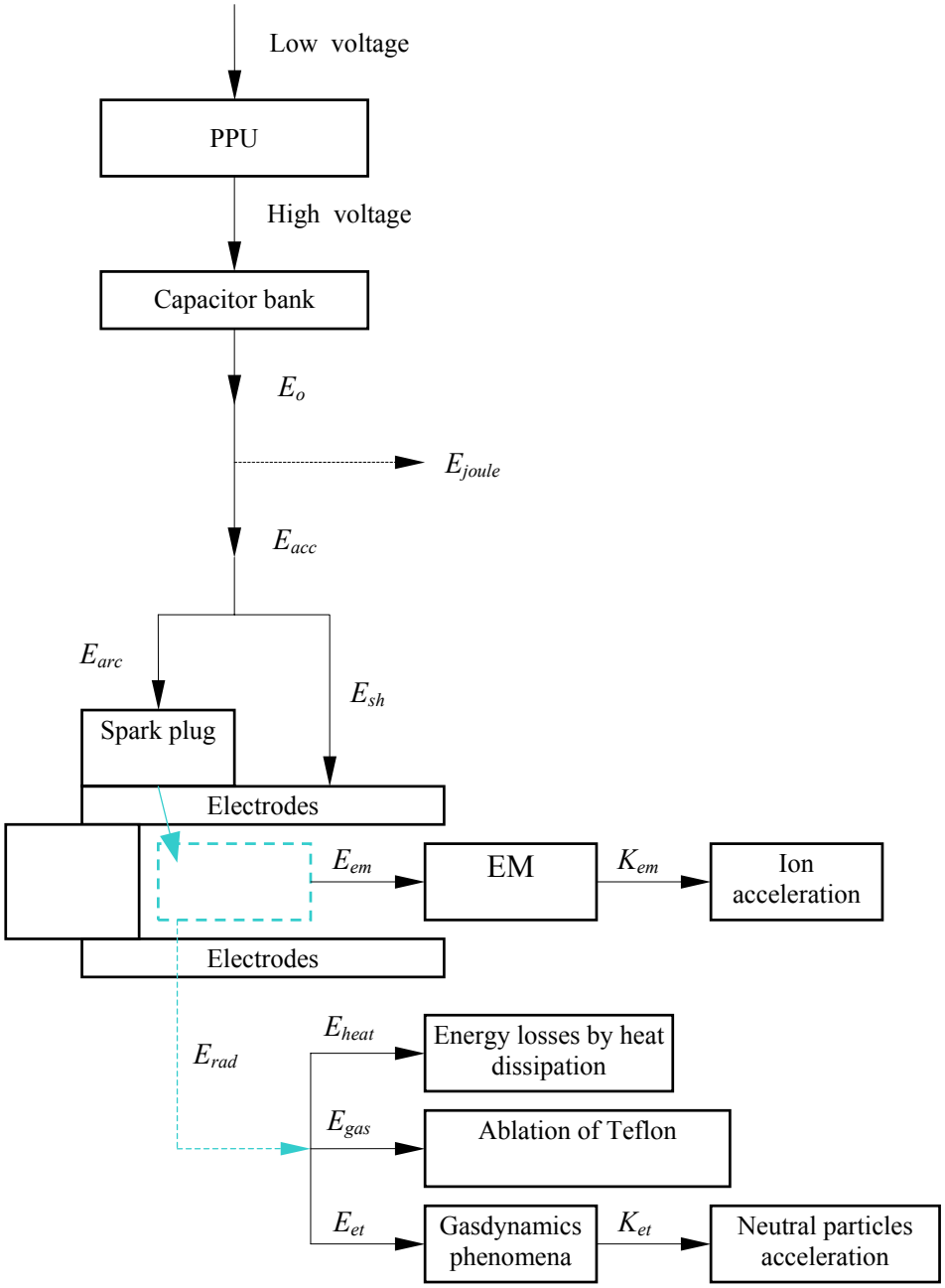

Figure 2. Energy balance of a typical APPT.

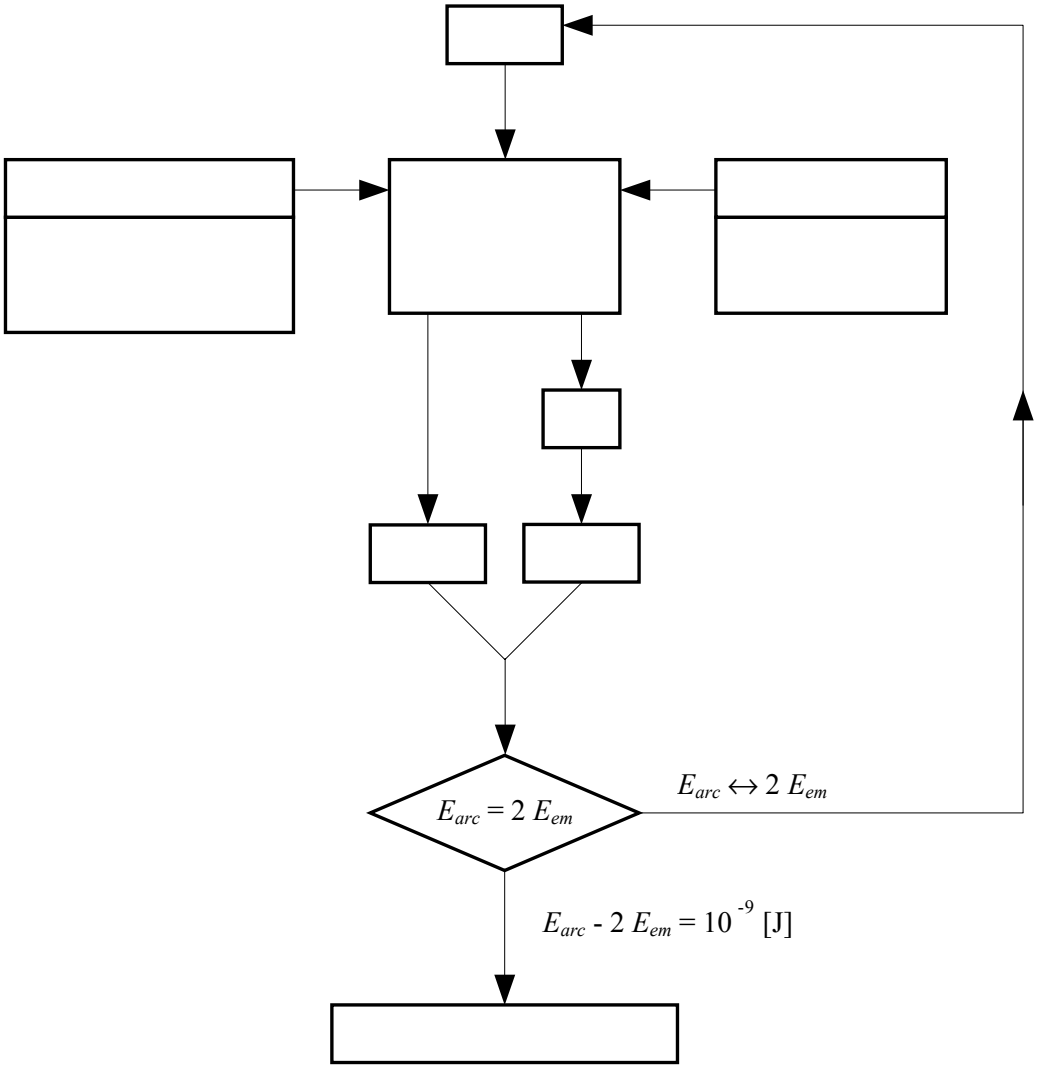

Figure 4. Determination of the ideal arc thickness.

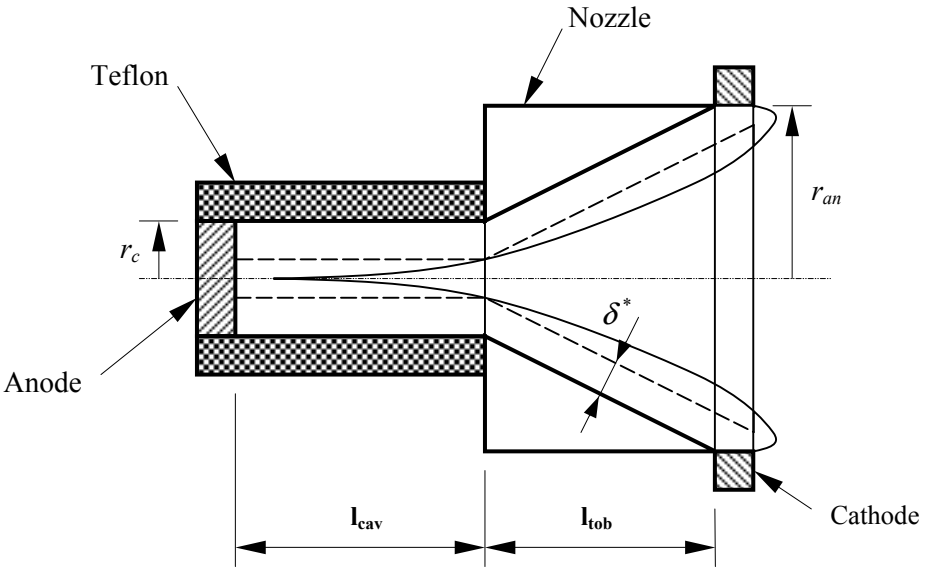

Figure 5. Configuration of the PPT-4 module.

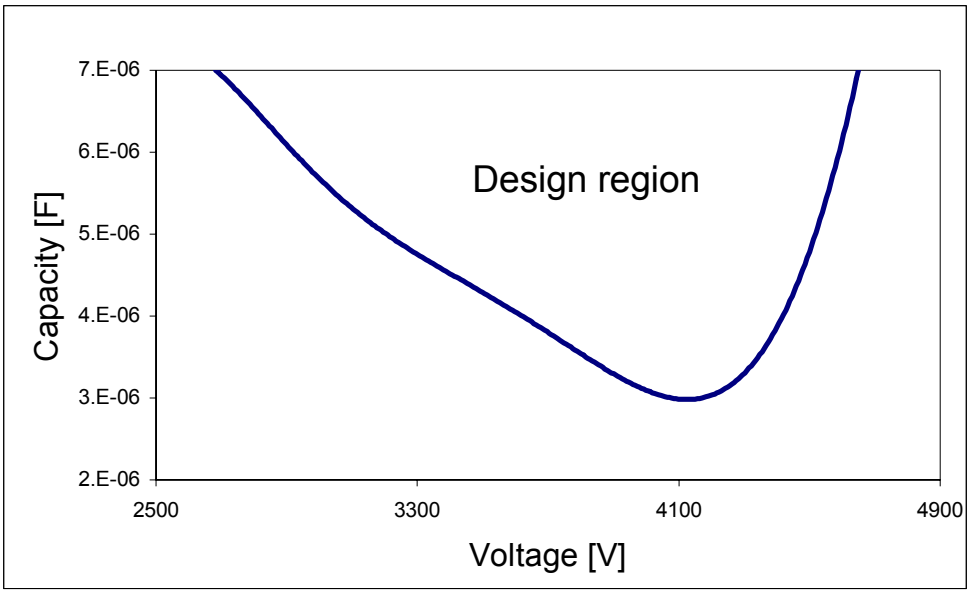

Fig. 7. Intersection region.

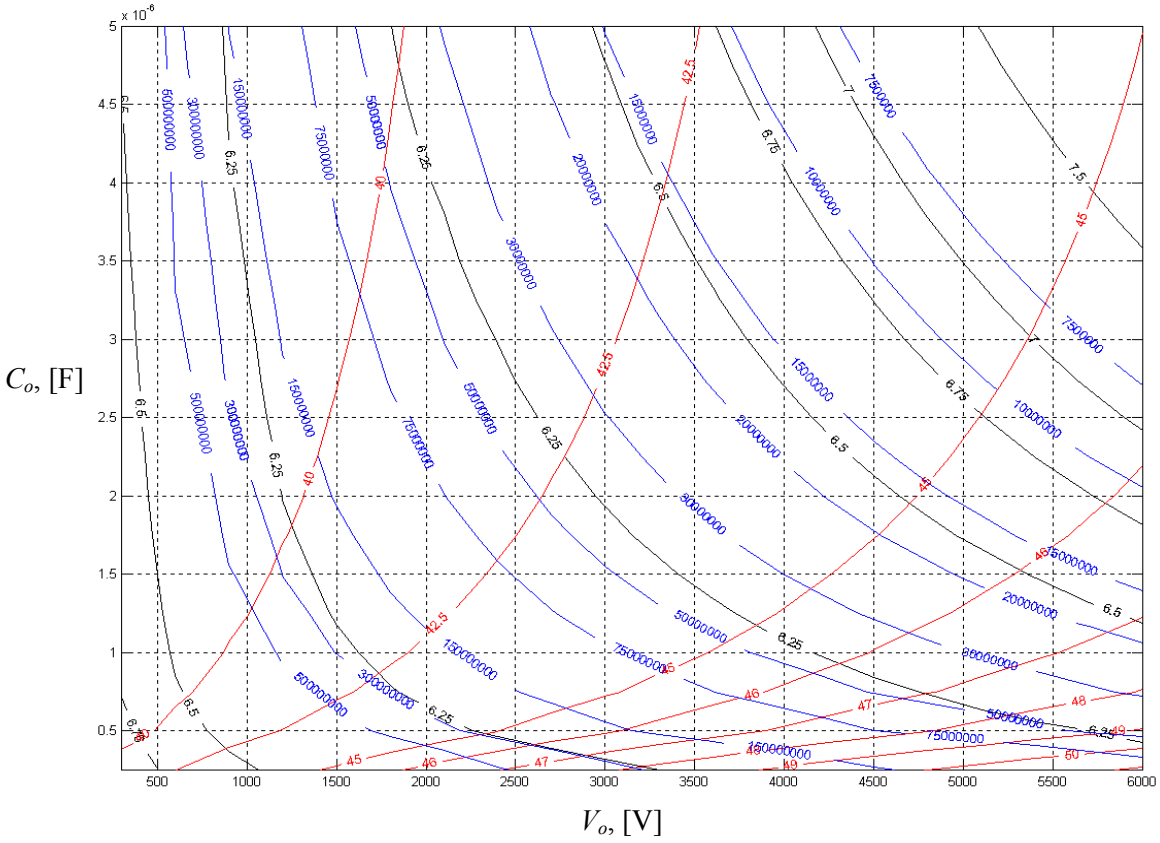

Figure 6. P4S-1 design map: mass [kg] (black), required bus power [W] (red), number of pulses (blue)